7. Babich JW, Graham W, Barrow SA, et al. Technetium-99m-labeled chemotactic peptides: comparison with indium-111-labeled white blood cells for localizing acute bacterial infection in rabbit. *J Nucl Med* 1993;34:2176–2181.
8. Peers SH, Tran LL, Eriksson SJ, Ballinger J, Goodbody AE. Imaging a model of colitis with RP128, a $^{99m}$Tc chelated tuftsin antogonist. *J Nucl Med* 1995;36:114P.
9. Moyer BR, Vallabhajosula S, Lister-James J, et al. Development of a white blood cell specific technetium-99m imaging agent from PF-4 for detecting infection [Abstract]. *J Nucl Med* 1995;36:(suppl)161P.
10. Ercan MT, Aras T, Unlenen E, Unlu M, Unsal IS, Hascelik Z. Technetium-99m-citrate versus $^{67}$Ga-citrate for the scintigraphic visualization of inflammatory lesions. *Nucl Med Biol* 1993;20:881–887.
11. Fischman AJ, Rubin RH, Khaw BA, et al. Detection of acute inflammation with indium-111-labeled nonspecific polyclonal IgG. *Semin Nucl Med* 1988;18:335–344.
12. Oyen WJ, Claessens RA, van der Meer, et al. Indium-111-labeled human nonspecific immunoglobulin G: a new radiopharmaceutical for imaging infectious and inflammatory foci. *Clin Infec Dis* 1992;14:1110–1118.
13. van der Laken J, Boerman OC, Oyen WJG, et al. Recombinant human interleukin-1: a potential agent to image infectious foci [Abstract]. *Eur J Nucl Med* 1994;21:790.
14. Thakur ML, DeFulvio J, Park CH, et al. Technetium-99m-labeled proteins for imaging inflammatory foci. *Nucl Med Biol* 1991;18:605–612.
15. Juweid M, Strauss HW, Yaoita H, Rubin RH, Fischman AJ. Accumulation of immunoglobulin G at focal sites of inflammation. *Eur J Nucl Med* 1992;19:159–165.
16. Solter D, Knowles BV. Monoclonal antibodies defining a stage-specific mouse in ionic antigen (SSEA-1). *Proc Natl Acad Sci USA* 1978;75:5565–5569.
17. Leibert N, Jaffe R, Taylor RJ, et al. Detection of SSEA-1 on human renal tumors. *Cancer* 1987;59:1404–1408.
18. Fox N, Damjanov I, Knowles BV, et al. Immunohistochemical localization of mouse stage-specific in ionic antigen-1 in human tissue and tumor. *Cancer Res* 1983;43:669–678.
19. Ballou B, Jeffe R, Taylor RJ, et al. Tumor radioimmuno location: differential antibody retention by antigenic normal tissue and tumor. *J Immunol* 1984;132:2111–2116.
20. Barclay NA, Birkeland ML, Brown MH, et al, eds. In: *The leukocyte antigen facts book*. New York: Academic Press; 1990:138.
21. Thakur ML, Lee J, DeFulvio J, Richard MD, Park CH. Human neutrophils: evaluation of adherence, chemotaxis and phagocytosis, following interaction wth radiolabeled antibodies. *Nucl Med Commun* 1990;11:37–43.
22. Thakur ML, Thiagarajan P, White F III, Park CH, Maurer PH. Monoclonal antibodies for specific cell labeling: considerations, preparations and preliminary evaluation. *Nucl Med Biol* 1987;14:51–58.
23. Thakur ML, DeFulvio JD. Technetium-99m-labeled monoclonal antibodies for immunoscintigraphy. Simplified preparation and evaluation. *J Immol Methods* 1991;137:217–24.
24. Thakur ML, DeFulvio JG. Determination of reduced disulfide groups in monoclonal antibodies. *Biotechniques* 1990;8:512–516.
25. Snyder WS, Ford MR, Warner GG, Watson SB. Nuclear Medicine/MIRD Pamphlet. New York: The Society of Nuclear Medicine, 1975.
26. Thomas SR, Maxon HR, Keriakes JG. In vivo quantitation of lesion radioactivity using external counting methods. *Med Phys* 1976;3:253–255.
27. Ashwell G, Hartfor J. Carbohydrate-specific receptors of the liver. *Ann Rev Biochem* 1982;51:531–554.
28. Halpern SE, Hagan PL, ChenA, et al. Distribution of radiolabeled humand and mouse monoclonal IgM antibodies in murine model. *J Nucl Med* 1988;29:1688–1696.
29. Becker W, Repp R, Hansen HJ, Goldenberg DM, Wolf F. Binding characteristics and kinetics of a new technetium-99m-antigranuleocyte FAB'-fragment (Leukoscan) [Abstract]. *J Nucl Med* 1995;36:208.
30. Thakur ML, Li J, Binoy C, et al. Transient neutropenia: neutrophil distribution and replacement. *J Nucl Med* 1996;37:489–494.
31. Rannine GH, Thakur ML, Ford WL. Indium-111-labeled lymphocytes: preparation, evaluation and comparison with $^{51}$Cr lymphocytes in rats. *Clin Exper Immunol* 1977;29:509–514.
32. Andres RY, Shubiger PA, Tiefenauer L, et al. Immunoscintigraphic imaging of inflammatory lesions: concept, radiolabeling and in vitro testing of a granulocyte specific antibody. *Eur J Nucl Med* 1988;13:582–586.
33. Hasler pH, Seybold K, Andres RY, Locher JT, Shubiger PA. Immunoscintigraphic imaging of inflammatory lesions: pharmacokinetics and estimated absorbed radiation dose in man. *Eur J Nucl Med* 1988;13:594–597.

# Left Ventricular Ejection Fraction: Comparison of Results from Planar and SPECT Gated Blood-Pool Studies

Marissa L. Bartlett, Gopal Srinivasan, W. Craig Barker, Anastasia N. Kitsiou, Vasken Dilsizian and Stephen L. Bacharach
*Department of Nuclear Medicine, National Institutes of Health, Bethesda, Maryland*

Global ejection fraction (EF) from planar gated blood-pool (GBP) imaging is a widely accepted measure of cardiac function. It has been suggested that planar GBP could be replaced by SPECT. In this article, we compare counts-based global EF measured from SPECT and planar images and investigate reasons for discrepancies between the two. **Methods:** Twenty-three subjects were imaged with both planar and SPECT GBP. SPECT short-axis slices were projected to create reprojected images. Reprojected SPECT (rSPECT) images were created in both the true long-axis view and also in a view typical of planar studies (found to be 60° from the true long-axis). Thus, angle of view effects on global EF could be investigated. In addition, we studied the effects of background and attenuation. **Results:** Long-axis rSPECT EF correlated well with planar EF ($r = 0.89$) but EF values were significantly higher for rSPECT than for planar (slope = 1.4, intercept = −8 EF units; $p < 0.001$). We found that background correction may not be necessary with rSPECT, but neither background nor attenuation explained the observed discrepancy between rSPECT and planar EFs. This discrepancy was found to be caused by atrial overlap in the planar image and disappeared when the SPECT slices were reprojected at the same angle of view as the planar images. **Conclusion:** Global EF can be easily measured from rSPECT GBP images. Long-axis rSPECT EFs are, however, greater than planar EFs by a factor of 1.4 because atrial overlap causes a significant drop in planar EF in planar images. These results suggest that (long-axis) rSPECT EFs may be more accurate than planar EFs.

**Key Words:** ejection fraction; SPECT gated blood-pool imaging; left ventricular function

**J Nucl Med 1996; 37:1795–1799**

Planar gated blood pool (GBP) studies provide valuable clinical information about myocardial wall motion and function. Regional wall motion is usually assessed visually. Global function is assessed principally by the ejection fraction (EF), a quantitative calculation of the change in measured blood-pool counts over the cardiac cycle. Global EF from planar GBP is widely used and of proven clinical significance (*1–4*). It has been suggested that planar GBP could be replaced by SPECT GBP (*5,6*). SPECT has the advantage of providing three-dimensional information which should improve assessment of regional wall motion (*7*) and may also allow the calculation of regional EFs (*8*). A primary practical concern, however, is whether global ejection fraction can be calculated easily and reliably from SPECT data.

The calculation of global EF from SPECT GBP has almost always been performed using a geometric method (*6–11*), in which left ventricle (LV) volume is found by estimating the edges of the LV blood pool in successive slices. This contrasts

Received Dec. 27, 1995; revision accepted Mar. 22, 1996.
For correspondence or reprints contact: Stephen Bacharach, PhD, National Institutes of Health, Dept. of Nuclear Medicine, Bldg. 10, Room 1C401, Bethesda, MD 20892-1180.

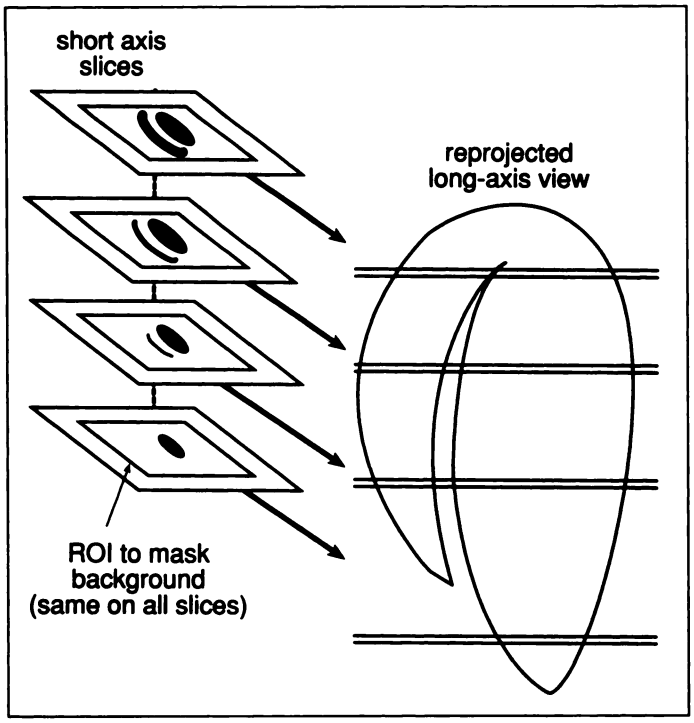


**FIGURE 1.** Reprojection of short-axis slices from SPECT GBP. Each short-axis slice is projected from posterior to anterior to provide one row in the reprojected image. (Four representative short-axis slices are shown. In a typical heart, a total of 20 to 25 slices are reprojected.)

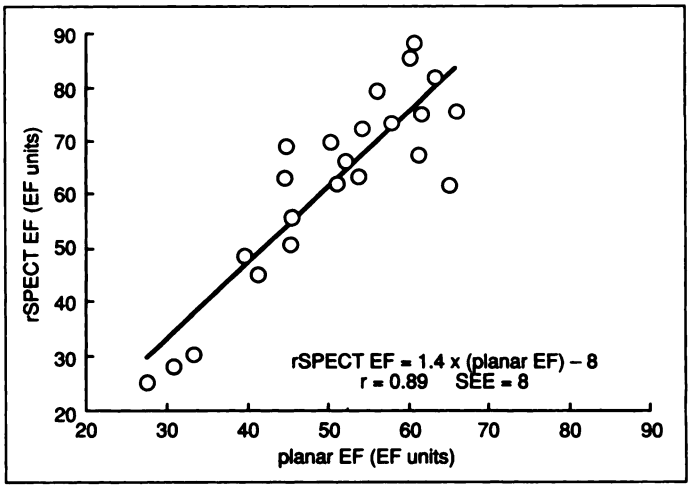


**FIGURE 2.** EF from rSPECT GBP versus EF from planar GBP with background correction calculated from 23 patients. The rSPECT images were projected at their true long-axis.

with the counts-based method, established in planar GBP imaging, in which LV volume is taken to be proportional to the measured counts in an LV region. The counts-based method obviates the need to accurately estimate edges, a notoriously difficult task given the count-poor, low-resolution nature of nuclear medicine images. Cross et al. (*12*) were among the few investigators to use a counts-based method with SPECT data. However, their primary goal was to investigate the use of PET in GBP imaging. They also calculated regional rather than global EF.

We wished to investigate the measurement of global EF from SPECT GBP images using the counts-based method. There were two possible approaches to this measurement: (a) the short-axis slices could be processed separately, with regions drawn on each slice at each time point or (b) the set of short-axis slices could be reprojected to give a single long-axis projection image at each time point. We chose to use reprojected SPECT (rSPECT) images for the following two reasons. First, processing the SPECT images slice-by-slice would require more regions per time point. Since the reprojected image is created by summing the counts in the slices, it is less noisy than any individual slice. Even if regions are generated by an automatic algorithm, the creation of more regions on relatively noisier slices is likely to result in greater variability, when calculating EF from separate slices. Second, rSPECT provides a more direct comparison with planar GBP which is, of course, also acquired by projection at one angle. Thus, rSPECT may provide insights into factors which influence planar global EF (the current clinical "gold standard").

## MATERIALS AND METHODS

### Patients

Twenty-three patients were studied (20 men, 3 women; age 19–74 yr; mean age 55 yr). Nineteen patients had coronary artery disease, one had hypertension and three had valvular disease. Patients abstained from all cardiac medications for 24–48 hr preceding the study. Each patient was injected with 25 mCi $^{99m}$Tc (after Sn pyrophosphate administration) and then imaged using both planar and SPECT techniques. The planar study was performed before the SPECT study in nine patients and after in 14. Average time between the two studies was approximately 1 hr (longest time 2 hr). Planar images were collected on a small field of view gamma camera with a pixel size of 2.22 mm. Images were acquired for 8–10 min in the LAO position to give the best ventricular separation, and with a caudal tilt applied to give the view most closely approximating the long-axis. SPECT images were collected on an dual-head camera (heads at 90°), with pixels ranging from 3.13- 4.56 mm and a reconstructed image resolution of 13 mm. Data were acquired for 20 min at 3° steps over 180° from the 45° RAO to the 45° LPO. Both planar and SPECT results were sorted into 16 images over the cardiac cycle, gated from the electrocardiogram, starting at end-diastole (ED).

The SPECT images were reoriented into short-axis slices, each one pixel thick. To produce a long-axis rSPECT image, data were reprojected perpendicular to the short-axis slices, as follows:

1. All the short-axis slices were rotated to optimize separation between the ventricles.
2. A simple rectangular region was positioned around both ventricles, and values outside this region were set to zero: this provided consistent, but incomplete, masking of background.
3. The activity in each slice was summed from back to front of the blood pool and thus contributed one row to the reprojected image.

The result was one vertical long-axis reprojection image of the blood pool for each time point (Fig. 1). It should be noted that this view could not, in general, be obtained with a planar camera.

For both planar and reprojected SPECT, EF was calculated by the standard two-region, background-corrected method (*13*). To reduce noise, ED and end-systole (ES) counts were taken from filtered time-activity curves (TACs) rather than directly from single images. That is, regions were drawn manually around the LV at ED and ES, and a background region was drawn on the ED image (lateral and adjacent to the LV). The ED and ES regions were then used to generate TACs, each of which was fit with a two harmonic Fourier series, and the value at ED or ES, as appropriate, was used in calculating the EF.

### Background

Background activity may be extremely low in rSPECT images since it is easy to mask much of the image outside the heart before

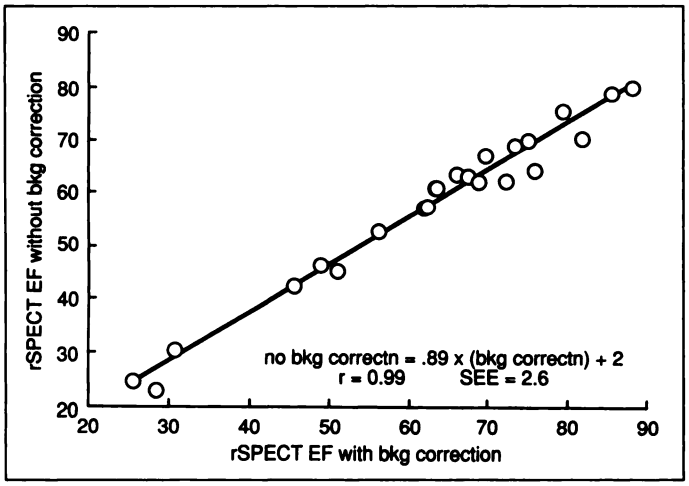


**FIGURE 3.** EF calculated from long-axis rSPECT GBP images without background correction versus with background correction for 23 patients.

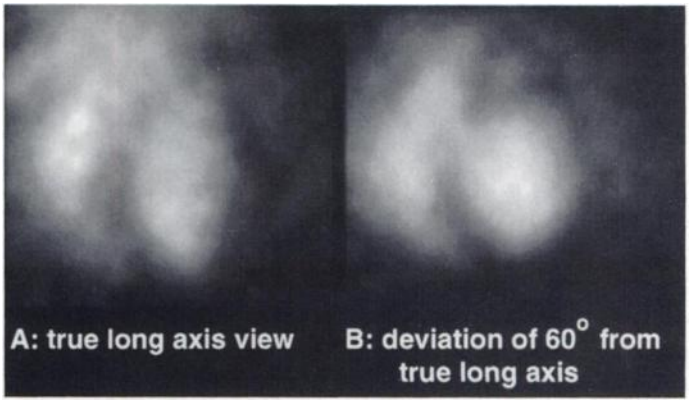


**FIGURE 4.** An ED blood pool is shown, using the reprojected SPECT technique. (A) Short-axis slices were reprojected perpendicular to the true long-axis. (B) Short-axis slices were reprojected at an angle 60° from perpendicular to the true long-axis (the typical projection angle seen in planar imaging when a caudal tilt was applied).

reprojection. To check this effect, we calculated rSPECT EF with and without background correction.

### Attenuation

To investigate the effects of attenuation on rSPECT EFs, we used a PET carbon monoxide ($^{11}CO$) GBP study. PET images were collected on a scanner with 1.7 mm pixels, a slice spacing of 5.1 mm and an image resolution of 7 mm. Regions were drawn manually around the LV on the transaxial slices. Since the regions were drawn on tomographic slices before projection, no background corrections were required. PET images were corrected for attenuation; therefore, EF measured from the PET GBP was not affected by attenuation. Additionally, we used the attenuation map to produce the same GBP slice with SPECT-like attenuation. This was done by scaling the PET attenuation values to correspond to 140 keV, before projecting the PET LV activity through these attenuation values. Projections were calculated at 120 different angles and then reconstructed to produce the same slice, now with SPECT attenuation. Hence, the EF from the same tomographic slice could be measured, with and without the effects of attenuation.

### Angle of View

Caudal tilt is applied to planar GBP studies to bring the LV images closer to a long-axis view. However, the geometry of the patient and the gamma camera usually prevents the use of a sufficiently large caudal tilt, so planar images often deviate from a true long-axis view. To investigate the effect of this deviation, we created rSPECT images in views other than the true long-axis. For 10 of the 23 patients, we produced reprojected images which deviated by 0°, 15°, 30°, 45°, 60° and 75° from the true long-axis.

We suspected that the EF would be different for nonlong-axis views because the atria drop behind the ventricles in such views and contribute counts to the LV regions. To test this hypothesis, for one angle, we masked the atria before reprojecting to a nonlong-axis view. This was accomplished by using amplitude images of long-axis slices to visually identify atrial activity. These areas of atrial activity were set to zero in the short-axis images before reprojection.

Since SPECT slices can be projected into a true long-axis view for each patient, the angle of view is generally different for planar and rSPECT images. This causes the perceived length of the LV to differ. We compared angles of view by measuring the caudal tilt applied when collecting planar data and by recording the specific angle by which SPECT data were rotated to obtain a true long-axis view. By manually selecting points corresponding to base and apex, we also estimated the length of the LV blood pool at ED from matched rSPECT and planar images.

## RESULTS

In Figure 2, rSPECT EFs are plotted against planar EFs, both calculated with background correction. The relationship is linear with a good correlation ($r = 0.89$), although the s.e. of the estimate (8 EF units) indicates some variability. Most importantly, rSPECT EFs are consistently higher than planar EFs: the slope is $1.4 \pm 0.16$ (significantly different from 1; $p < 0.001$). We studied the effects of background activity, attenuation and angle of view on rSPECT global EF values, seeking to explain this difference.

### Background

For all 23 patients, the background fraction was calculated as background counts divided by LV counts at ED. The average background fraction for rSPECT (19% ± 7%) was significantly lower than for planar (48% ± 5%; $p < 0.001$). In fact, the background was so low for rSPECT that omitting the background correction introduced practically no additional variability into the EF values. This can be seen by plotting rSPECT EF with background correction against rSPECT EF without background correction (Fig. 3). With no background correction, the mean rSPECT EF was significantly lower (58 EF units versus 68 EF units; $p < 0.001$), but the correlation coefficient was 0.99 and the s.e.e. was only 2.6 EF units. Furthermore, if planar EFs

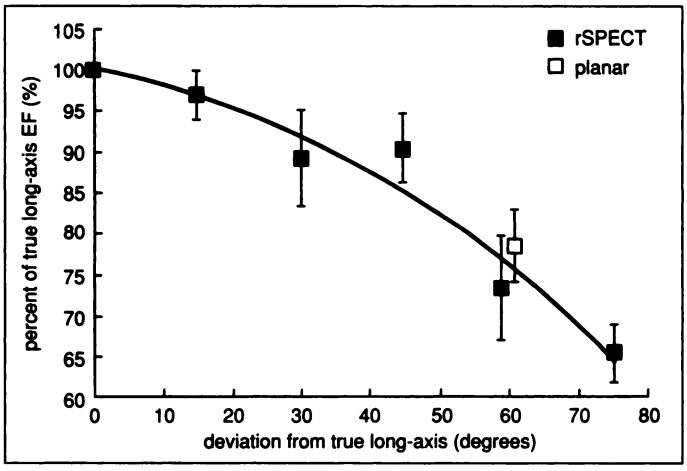


**FIGURE 5.** EF calculated from rSPECT GBP. Percent change in ejection fraction versus angular deviation from the true long-axis of the reprojected image. Each error bar indicates the s.d. of an estimate of the mean.

are again plotted against rSPECT EFs, without SPECT background correction, the s.e.e. is unchanged at eight EF units.

As noted above, rSPECT EFs dropped significantly when the background correction was omitted. Planar EF values (51 ± 11 EF units), however, were still significantly lower than uncorrected rSPECT EFs (58 ± 16 EF units; $p < 0.001$). Differences in background therefore do not explain the discrepancy in EF between the two techniques.

### Attenuation

We calculated EF from a PET-based GBP slice, once including the effects of SPECT attenuation and once with attenuation corrected for. The EFs were 35 and 34 EF units, respectively. Attenuation, thus, had almost no effect on global rSPECT EF.

### Angle of View

On average, the caudal tilt applied in collecting planar data was 11° (±2°), while the angle by which SPECT data were rotated to obtain the long-axis view averaged 69° (±9°). These numbers are significantly different ($p < 0.001$) and suggest that the planar images are about 60° from a long-axis view. Because of this difference in angle of view, the LV blood pool appeared shorter in planar ED images than in matching rSPECT ED images (62 ± 12 mm and 84 ± 8 mm, respectively; $p < 0.001$).

For 10 patients, EFs from long-axis rSPECT images were compared with EFs from the same SPECT images reprojected to nonlong-axis views. Figure 4 shows an example of one rSPECT image, in the true long-axis view and also at a deviation of 60° from the long axis. For each patient, the EF from the nonlong-axis view was calculated as a percentage of the long-axis EF. Figure 5 shows these percentages plotted against each angle of view, averaged over the 10 patients. Thus, the long-axis view (0° deviation from true long-axis) by definition gives 100% and, for example, images which deviated from the long axis view by 15° gave lower EFs (on average 97% of the long-axis values).

As the projection angle deviated from the long axis view, the rSPECT EF value dropped consistently. For example, the rSPECT EF dropped significantly from an average of 69 EF units at the true long-axis to 50 EF units ($p < 0.01$) at a 60° deviation from true long-axis. At this deviation, which is the average angle of view for planar studies, rSPECT EF (50 EF units) was very similar to planar EF (53 EF units, p = n.s.). The reason for this decrease in EF was sought by masking atrial counts before reprojecting again at 60° from the long-axis. With the atria masked, rSPECT EF no longer dropped with projection angle (rSPECT EF = 69 EF units at true long-axis; rSPECT EF = 72 EF units at 60° with atria masked, p = ns). Therefore, it appears to be the presence of overlapping atrial counts in the planar studies which caused planar EF to be lower than true long-axis rSPECT EF.

## DISCUSSION

Global EF was calculated from planar and from rSPECT images using a counts-based method. We found that the EFs correlated well but with a slope which was significantly different from one. We investigated the effects of background activity, attenuation and angle of view to identify reasons for this difference in EF values.

### Background

Background was low in rSPECT images, so that omitting background correction in calculating EF introduced no extra variability. Absolute rSPECT EF values did drop somewhat when background correction was not performed, but not enough to explain the difference in EF values between rSPECT and planar.

For routine clinical use, the difference in rSPECT EF associated with omitting the background correction may not be considered important. The notable finding here is that eliminating background correction did not increase the s.e.e. of EF values. As long as an appropriate normal range is established, therefore, background correction may not be necessary for calculating rSPECT EF. The situation is extremely different for planar imaging where omission of the background correction might greatly increase EF variability.

### Attenuation

We found that attenuation has little effect on global EF values for rSPECT. This result is based on calculations from only a single patient. Our comparison of global EF, however, with and without attenuation was accurate, since the correct attenuation map for that patient was used. Also, our finding is in agreement with those of Cross et al. (*12*). Our results clearly do not provide exhaustive, quantitative information about the effect of attenuation on global EF from rSPECT. They do, however, indicate that the size of this effect may be expected to be very small.

The fact that rSPECT global EF is unaffected by attenuation does not mean that attenuation is negligible in SPECT images. Reintroducing SPECT attenuation in a PET GBP slice caused the measured LV counts to drop by a factor of four. The global EF was not changed because LV counts at ED and ES were reduced by the same factor. However, in calculating regional, as opposed to global, EF from SPECT slices, attenuation may well be an important factor.

### Angle of View

Finally, we established that the ability to reliably produce true long axis views, which is possible with rSPECT but not with planar imaging, is of great importance. Planar images were found to deviate from a true long-axis view by an average of about 60°, even with optimal caudal tilt. Such a deviation was found to result in a significant and substantial decrease in measured EF because of associated atrial overlap. This result was confirmed by showing that masking the atria before projecting, resulted in nonlong-axis EFs which were indistinguishable from the true long-axis EFs.

In general, previous investigators who compared SPECT and planar GBP EFs used geometric rather than counts based methods. It is therefore not possible to compare our results directly with theirs. Miller et al. (*14*) used the counts-based method to compare planar EFs with EFs from reprojected tomographic images ($^{15}$CO PET). However, as they wished to mimic planar studies as closely as possible, they reprojected the PET images with a caudal tilt of only 12°, thereby precluding the possibility of confirming our observations about long-axis views, from their data.

Our results suggest that EFs from rSPECT may be more accurate than planar EFs, because of the suboptimal angle of view and resultant atrial overlap associated with planar imaging. This effect may be diminished by the atrial attenuation in a planar study. Planar EFs might be corrected for this atrial overlap, using a relationship such as that in Figure 2. However, the degree of atrial overlap is probably different for each patient, so the correction required would also be different. It is unlikely, therefore, that a single equation could be used to correct the planar EFs.

The relative convenience of planar and SPECT GBP will vary for different centers. SPECT obviously requires more computer power for reconstruction and reorientation of the images. A SPECT study also requires more time than a single

planar study. However, collecting three views is routine in planar studies. In our laboratory, we typically collect three rest planar studies in approximately the time required for our resting SPECT acquisitions (about 30–35 min).

## CONCLUSION

Global EF can be easily measured from reprojected SPECT GBP images using a counts-based method. This technique yields background activity levels that are so low that background correction is probably not necessary. In addition, it seems that global EF is not measurably affected by the attenuation inherent in SPECT imaging. Finally, rSPECT EFs were greater than planar EFs by a factor of 1.4, and our results suggest that the SPECT EFs may be more accurate than those from planar images. The discrepancy arises because the angle of view of planar images is sufficiently far from the long-axis to cause a significant drop in the measured EF, due to atrial overlap. The exact amount by which the EF is decreased will vary from patient to patient. rSPECT avoids this problem since images can always be presented in the true long-axis view.

## REFERENCES


1. Borer JS, Bacharach SL, Green MV, Kent KM, Epstein SE, Johnston GS. Real-time radionuclide cineangiography in the noninvasive evaluation of global and regional left ventricular function at rest and during exercise in patients with coronary-artery disease. *N Engl J Med* 1977;296:839–844.
2. Gibbons RJ. The use of radionuclide techniques for identification of severe coronary disease. *Curr Probl Cardiol* 1990;15:301–352.
3. Rocco TP, Dilsizian V, Fischman AJ, Strauss HW. Evaluation of ventricular function in patients with coronary artery disease. *J Nucl Med* 1989;30:1149–65.
4. Dilsizian V, Rocco TP, Bonow RO, Fischman AJ, Boucher CA, Strauss HW. Cardiac blood-pool imaging. II. Applications in noncoronary heart disease. *J Nucl Med* 1990;31:10–22.
5. Moore ML, Murphy pH, Burdine JA. ECG-gated emission computed tomography of the cardiac blood pool. *Radiology* 1980;134:233–235.
6. Corbett JR, Jansen DE, Lewis SE, et al. Tomographic gated blood pool radionuclide ventriculography: analysis of wall motion and left ventricular volumes in patients with coronary artery disease. *J Am Coll Cardiol* 1985;6:349–358.
7. Gill JB, Moore RH, Tamaki N, et al. Multigated blood-pool tomography: new method for the assessment of left ventricular function. *J Nucl Med* 1986;27:1916–1924.
8. Cerqueira MD, Harp GD, Ritchie JL. Quantitative gated blood pool tomographic assessment of regional ejection fraction: definition of normal limits. *J Am Coll Cardiol* 1992;20:934–941.
9. Stadius ML, Williams DL, Harp G, et al. Left ventricular volume determination using single-photon emission computed tomography. *Am J Cardiol* 1985;55:1185–1191.
10. Underwood SR, Walton S, Laming PJ, et al. Left ventricular volume and ejection fraction determined by gated blood pool emission tomography. *Br Heart J* 1985;53: 216–222.
11. Lu P, Liu X, Shi R, Mo L, Borer JS. Comparison of tomographic and planar radionuclide ventriculography in the assessment of regional left ventricular function in patients with left ventricular aneurysm before and after surgery. *J Nucl Cardiol* 1994;1:537–545.
12. Cross SJ, Lee HS, Metcalfe MJ, Norton MY, Evans NTS, Walton S. Assessment of left ventricular regional wall motion with blood-pool tomography: comparison of $^{11}$CO PET with $^{99m}$Tc-SPECT. *Nucl Med Commun* 1994;15:283–288.
13. Reiber JHC, Lie SP, Simoons ML, et al. Clinical validation of fully automated computation of ejection fraction from gated equilibrium blood-pool scintigrams. *J Nucl Med* 1983;24:1099–1107.
14. Miller TR, Wallis JW, Landy BR, Gropler RJ, Sabharwal CL. Measurement of global and regional left ventricular function by cardiac PET. *J Nucl Med* 1994;35:999–1005.


# Reappraisal of Quantitative Esophageal Scintigraphy by Optimizing Results with ROC Analyses


Klaus Tatsch, Winfried A. Voderholzer, Martin J. Weiss, Wilhelm Schröttle and Klaus Hahn

*Departments of Nuclear Medicine and Internal Medicine, Medizinische Klinik Innenstadt, University of Munich, Germany*



This study investigates whether systematic analyses of methodological issues contribute to improve and renew the diagnostic role of quantitate esophageal scintigraphy. **Methods:** Forty-seven patients with normal (n = 26) and pathologic (n = 21) esophageal function were studied with scintigraphy and manometry, using the latter findings as the gold standard. Scintigraphic data were analyzed by receiver operator characteristic (ROC) methods to: establish the optimal decision threshold for six different quantitative parameters, evaluate their inherent discrimination capacity and compare liquid compared with solid bolus data. **Results:** Quantitative parameters have shown remarkable differences in their potential to discriminate between normal and pathologic findings (percentage of emptying at definite time points > mean time > transit time > mean transit time > $T_{max}$). Sensitivity of 95% at a specificity of 96% was the optimum obtained. At comparable specificity levels, solid bolus studies generally demonstrated higher sensitivity than liquid bolus studies. **Conclusion:** The diagnostic performance of optimized esophageal scintigraphy is close to that of manometry. Our findings do not only renew the role of esophageal scintigraphy as an accurate screening test for esophageal motility disorders but also invalidate recent reservations about the diagnostic potential of this method.



**Key Words:** esophageal scintigraphy; quantification; ROC analyses

**J Nucl Med 1996; 37:1799–1805**

Received Jul. 31, 1995; revision accepted Mar. 6, 1996.



For correspondence or reprints contact: Klaus Tatsch, MD, Dept. of Nuclear Medicine, Klinikum Grosshadern, University of Munich, Marchioninistr. 15, 81377 Munich, Germany.


In 1972, Kazem (*1*) reported on the use of various radiopharmaceuticals and a gamma camera to monitor swallowing. Since then, several investigators have established scintigraphic techniques for the evaluation of esophageal motility disorders (*2–10*). Although several drawbacks from previous methods have been solved by recent developments [i.e., condensed images for a more accurate depiction of esophageal events (*5,7,8,11–14*) or multiple swallow protocols to compensate for the intraindividual variation between repetitive swallows (*10,15*)], the diagnostic role of esophageal scintigraphy is still under discussion.

In earlier reports, several authors proposed that radionuclide transit studies are a sensitive screening test to detect esophageal motility disorders (*3,6,16*). Others concluded that esophageal scintigraphy is of limited use only (*17,18*), and some investigators even stated that this approach has almost no diagnostic significance (*19,20*).

There are several reasons that may account for the discrepant appraisal of esophageal scintigraphy, such as the obvious differences in the methodological approach. In this context, little attention focused on relevant issues such as: the kind of quantitative parameters used, how decision thresholds for discriminating normal compared with pathologic function were established, whether studies were performed with liquid or solid boluses or whether single compared with multiple-swallow protocols were applied to establish scintigraphic results.

The aim of this study was to determine whether or not further